Editors' Suggestion | Featured in Physics

Superallowed α Decay to Doubly Magic ^{100}Sn

K. Auranen,[1,*] D. Seweryniak,[1] M. Albers,[1] A. D. Ayangeakaa,[1,†] S. Bottoni,[1,‡] M. P. Carpenter,[1] C. J. Chiara,[1,2,§] P. Copp,[1,3] H. M. David,[1,‖] D. T. Doherty,[4,¶] J. Harker,[1,2] C. R. Hoffman,[1] R. V. F. Janssens,[5,6] T. L. Khoo,[1] S. A. Kuvin,[1,7] T. Lauritsen,[1] G. Lotay,[8] A. M. Rogers,[1,**] J. Sethi,[1,2] C. Scholey,[9] R. Talwar,[1] W. B. Walters,[2] P. J. Woods,[4] and S. Zhu[1]

[1]*Physics Division, Argonne National Laboratory, 9700 South Cass Avenue, Lemont, Illinois 60439, USA*
[2]*Department of Chemistry and Biochemistry, University of Maryland, College Park, Maryland 20742, USA*
[3]*Department of Physics and Applied Physics, University of Massachusetts Lowell, Lowell, Massachusetts 01854, USA*
[4]*University of Edinburgh, Edinburgh EH9 3JZ, United Kingdom*
[5]*Department of Physics and Astronomy, University of North Carolina at Chapel Hill, Chapel Hill, North Carolina 27599, USA*
[6]*Triangle Universities Nuclear Laboratory, Duke University, Durham, North Carolina 27708, USA*
[7]*Department of Physics, University of Connecticut, Storrs, Connecticut 06269, USA*
[8]*University of Surrey, Guildford GU2 7XH, United Kingdom*
[9]*Department of Physics, University of Jyvaskyla, P.O. Box 35, FI-40014 University of Jyvaskyla, Finland*

(Received 31 July 2018; revised manuscript received 7 September 2018; published 30 October 2018)

We report the first observation of the $^{108}\mathrm{Xe} \rightarrow {}^{104}\mathrm{Te} \rightarrow {}^{100}\mathrm{Sn}$ α-decay chain. The α emitters, ^{108}Xe [$E_\alpha = 4.4(2)$ MeV, $T_{1/2} = 58^{+106}_{-23}$ μs] and ^{104}Te [$E_\alpha = 4.9(2)$ MeV, $T_{1/2} < 18$ ns], decaying into doubly magic ^{100}Sn were produced using a fusion-evaporation reaction $^{54}\mathrm{Fe}(^{58}\mathrm{Ni}, 4n)^{108}\mathrm{Xe}$, and identified with a recoil mass separator and an implantation-decay correlation technique. This is the first time α radioactivity has been observed to a heavy self-conjugate nucleus. A previous benchmark for study of this fundamental decay mode has been the decay of ^{212}Po into doubly magic ^{208}Pb. Enhanced proton-neutron interactions in the $N = Z$ parent nuclei may result in superallowed α decays with reduced α-decay widths significantly greater than that for ^{212}Po. From the decay chain, we deduce that the α-reduced width for ^{108}Xe or ^{104}Te is more than a factor of 5 larger than that for ^{212}Po.

DOI: 10.1103/PhysRevLett.121.182501

The region around the self-conjugate doubly magic ^{100}Sn nucleus, located near the proton drip line [1], is one of the focal points of nuclear structure [2]. Recently, ^{100}Sn β decay was shown to exhibit the largest Gamow-Teller strength measured to date [3], and the first single-neutron excitation was identified in ^{101}Sn [4,5]. Another manifestation of the doubly magic nature of ^{100}Sn is the existence of an island of enhanced α emitters which decay towards the $Z = N = 50$ closed shells. In fact, the emission of heavier clusters such as ^{8}Be, ^{12}C, and ^{14}C was also proposed in this region [6–8]. A similar decay pattern can be found in the well-studied region near the stable doubly magic ^{208}Pb nucleus. In contrast to ^{208}Pb, valence protons and neutrons in nuclei near ^{100}Sn occupy the same orbitals, resulting in stronger proton-neutron interactions.

α decay is a fundamental nuclear decay mode. Despite scores of known α emitters, calculating associated lifetimes remains a challenge [9]. The α-emission probability is the product of the formation probability of the α particle inside the nucleus (preformation factor) and its transmission through the Coulomb barrier. While the latter can be readily computed, the former requires microscopic calculations, in which the preformation can be viewed as the overlap between the initial-state wave function and those of the states in the daughter nucleus and of the outgoing α particle. Residual nucleon-nucleon interactions are an important ingredient in such calculations. Because of its simplicity, the α decay of ^{212}Po to its doubly magic ^{208}Pb daughter can be viewed as a benchmark for models of α emission [10]. In fact, it is the only known α decay to a doubly magic daughter. The only other decay of the same type involves ^{104}Te, which is located far from the line of stability and, prior to this work, had not been observed due to a very small production cross section and anticipated short half-life. It is noteworthy that this $^{104}\mathrm{Te} \rightarrow {}^{100}\mathrm{Sn}$ decay is also of particular interest because enhanced proton-neutron interactions could result in an unusually large preformation factor. Hence, a comparison between ^{212}Po and ^{104}Te provides a direct assessment of the role of these interactions in α-particle formation [11,12]. Such a superallowed α decay was proposed already in 1965 by Macfarlane and Siivola [13]. Experimentally, enhanced α decays have been observed near the $N = Z$ line in ^{105}Te [14,15], ^{106}Te [16,17], ^{110}Xe [16,17], and ^{114}Ba [17]. However, prior to this work, no information was available for any self-conjugate α emitters, where this effect should be the strongest.

In this Letter, the first observation of the new $N = Z$ isotopes ^{108}Xe and ^{104}Te, decaying into doubly magic ^{100}Sn, is reported. The measured decay properties are compared

with those in neighboring even-even nuclei. It is shown that, in at least one of these nuclei, the α-particle preformation factor is more than 5 times larger than that seen in ^{212}Po, suggesting superallowed α decay and resulting in one of the largest values among the α emitters near the $N = Z$ line and, in fact, in the entire nuclear chart.

The experiment was conducted at the ATLAS facility of Argonne National Laboratory using the Fragment Mass Analyzer (FMA) [18]. The expected half-life of ^{104}Te is of the order of a few nanoseconds [19], about a factor of a hundred shorter than the time of flight of reaction products through the separator. Therefore, the ^{54}Fe(^{58}Ni, $4n$)^{108}Xe reaction was chosen to produce ^{108}Xe instead. The latter decays into ^{104}Te, but is expected to live long enough to survive the flight through the FMA. The anticipated production cross section of ^{108}Xe is less than 1 nb, in the presence of background from other reaction channels corresponding to about 700 mb. In order to achieve the required selectivity, the recoil-decay correlation method was implemented to identify weakly produced α emitters. Self-supporting 450-μg/cm^2-thick ^{54}Fe targets were mounted on a rotating wheel in order to accommodate the high beam intensity. Downstream from the target wheel, a 20-μg/cm^2 stationary carbon foil was used to reset the charge-state distribution of the recoiling residues. The ^{58}Ni beam had a laboratory energy of 245 MeV and an average intensity of 32 particle nA (2×10^{11} ions/s). The total irradiation time was approximately 118 h. The FMA was set to collect fusion-evaporation residues (referred to as recoils below) with a mass number of 108 and a charge state of +26 or +27 through slits located at the focal plane. A position-sensitive parallel-grid avalanche counter (PGAC) measured mass-to-charge-state ratios of nuclei transported through the FMA. Behind the PGAC, the recoils were implanted into a 100-μm thick, 64×64 mm^2, 160×160 strip double-sided silicon detector (DSSD). Eight 300-μm thick, 4×7 cm^2 single-sided silicon detectors, each composed of seven strips, were placed upstream from the DSSD in a box geometry (referred to as the BOX detector below) to detect α particles escaping from the DSSD. Individual events from each detector were time stamped with a 100-MHz clock. An approximately 4-μs long trace was collected for each DSSD event in order to analyze pileup events. The energies deposited in the DSSD were extracted using a linear energy calibration obtained with an α source containing ^{240}Pu and ^{244}Cm isotopes (gain parameter) and with the observed ^{108}Te [$E_\alpha = 3314(4)$ keV [20]] α activity (offset parameter). The BOX detector was calibrated using the escaping ^{108}Te α particles. The α-decay recoil effect [21,22], as well as dead layer effects in both detectors, were accounted for in these calibrations.

In Fig. 1, all observed decay events correlated with a recoil event measured in the same pixel of the DSSD are displayed. An event was considered to be a recoil if (i) the

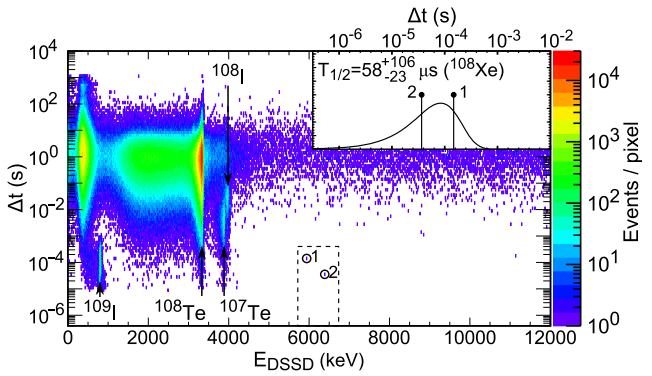

FIG. 1. Time difference between a recoil implantation and a subsequent decay event occurring in the same pixel of the DSSD as a function of the energy deposited by the decay event. Previously identified activities are labeled. The two events associated with the new activities are marked with numbers 1 and 2. The inset provides the time distribution of these events. The half-life of ^{108}Xe was extracted using the maximum likelihood method [23], and the solid line in the inset is the determined probability distribution function. The ordinate of the inset is arbitrary. See text for details on the region marked with a dashed line.

PGAC yielded $A = 108$, (ii) the energy registered in the DSSD was greater than 15 MeV, and (iii) a time-of-flight condition between the PGAC and the DSSD was satisfied. An event without a PGAC signal was considered to be a decay event. In Fig. 1, events arising from previously known activities are labeled. The high-energy background present in Fig. 1 is due to scattered beam and other implants, which were not vetoed by the PGAC. The two events, clearly separated from the background, marked with numbers 1 and 2, are shorter lived and more energetic than any known α emitter in this region. Furthermore, a particle was registered by the BOX detector in coincidence with both of these events; see Fig. 2. As can be seen in the inset of Fig. 2, the energy sum of the two coincident DSSD and

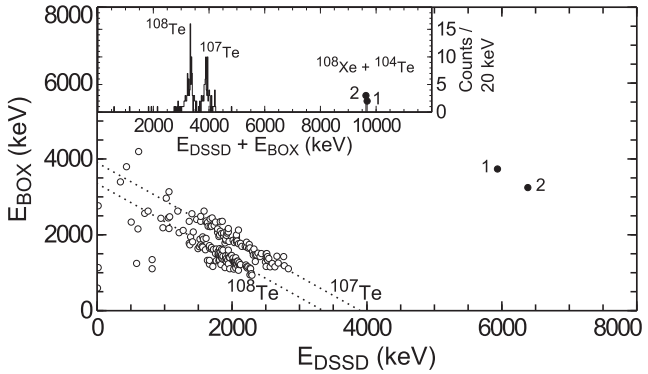

FIG. 2. Energies of coincident events observed within 250 ns in the DSSD and the BOX and in less than 1 ms after a recoil implantation. The two dashed lines correspond to the literature α-particle energies of ^{107}Te and ^{108}Te. The inset provides the energy sum (events of interest are adjusted vertically for clarity).

TABLE I. The ^{108}Xe → ^{104}Te → ^{100}Sn α-decay chains observed in the present study. E_α is the reconstructed α-particle energy and τ is the recorded decay time.

Chain	$E_\alpha(^{108}\mathrm{Xe})$ (MeV)	$E_\alpha(^{104}\mathrm{Te})$ (MeV)	$\tau(^{108}\mathrm{Xe})$ (μs)	$\tau(^{104}\mathrm{Te})$ (ns)
1	4.56(26)	4.73(24)	139	<20
2	4.23(20)	5.06(25)	28	<20

BOX events is nearly identical. By fitting and integrating the background in Fig. 1, it was found that less than 0.09 events can be attributed to random correlations in the region near the events of interest, marked with dashed lines in Fig. 1. Furthermore, the background is reduced by a factor greater than 400, once a coincidence event in the BOX is required. Given the nearly equal total energies and the low background, it is very unlikely that the two observed coincidence events are due to random correlations.

The energy deposited in the DSSD is too high to originate from a single escaping high-energy α particle, suggesting another origin. Consequently, event 1 (2) was interpreted as the α particle from ^{108}Xe stopped in the DSSD (BOX), rapidly followed by an α particle from ^{104}Te stopped in the BOX (DSSD). There are no events indicating the observation of both α decays with full energy in the DSSD. The deduced properties of these chains are listed in Table I and are discussed in detail below. Regardless of which α particle was stopped in the DSSD, the time difference between this DSSD event and the preceding recoil event, observed in the same pixel of the DSSD, reflects the decay time of ^{108}Xe. This time distribution is presented in the inset of Fig. 1. The ^{108}Xe half-life of 58^{+106}_{-23} μs was determined with the maximum likelihood method [23]. In order to extract the anticipated short half-life of ^{104}Te, DSSD traces corresponding to ^{108}Xe-^{104}Te pileup events were analyzed. In Fig. 3, the second derivatives of the recorded DSSD traces are displayed for each event and compared to differentiated reference double-decay traces with a delay varying from 0 to 60 ns between consecutive decays. The reference traces were obtained by taking an average trace recorded for the α decay of ^{108}Te from the same DSSD strips in which the events of interest were recorded, then scaling and delaying it before summing it with the original trace to simulate a sequence of two decays. The peak in the reference trace for $\Delta t = 20$ ns displays a broadening, which is not visible in the traces of events 1 and 2, implying a decay time shorter than 20 ns for both events, and resulting in an upper limit of 18 ns with a 68% probability for the ^{104}Te half-life. This is about a factor of 3 shorter than the reported half-life of ^{219}Pa [53(10) ns [24], 60^{+28}_{-15} ns [25]], making ^{104}Te the shortest-lived ground-state α emitter observed thus far [26].

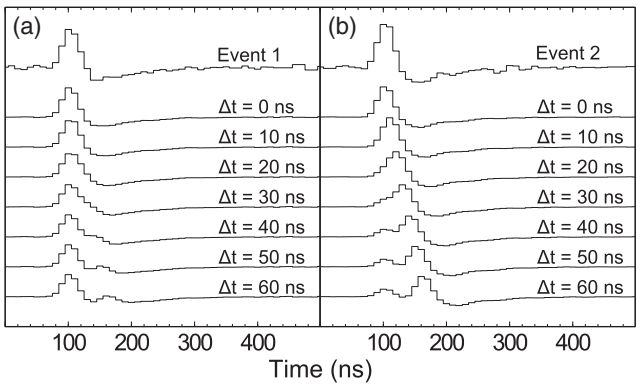

FIG. 3. The second derivative of the DSSD traces of events (a) 1 and (b) 2 compared to the second derivative of a reference double-decay trace (see text for details) with a time delay from 0 to 60 ns between the consecutive decays. The reference decay events with lower amplitude are escape events.

The ^{108}Xe and ^{104}Te α-particle energies were reconstructed from the energies deposited in the DSSD and the BOX detector. The energy registered by the DSSD is the sum of one full α-particle energy, one partial α-particle energy, and two α-decay recoil energies partially recorded [22]. The partition of the energy deposited in the DSSD depends sensitively on the implantation depth, which was deduced from the observed ^{108}Te escape events. A correction term was applied to account for the difference between the energy loss of the ^{108}Te α particles and that of the ^{108}Xe and ^{104}Te α particles in the dead layers of the DSSD and the BOX. The required ranges for α particles in silicon were computed using the ASTAR calculator [27], which is based on the ICRU Report 49 [28]. The α-particle energy reconstruction resulted in values of $E_\alpha(^{108}\mathrm{Xe}) = 4.4(2)$ MeV and $E_\alpha(^{104}\mathrm{Te}) = 4.9(2)$ MeV. The higher energy was assigned to ^{104}Te, based on systematics. The quoted uncertainty is dominated by the determination of the implantation depth.

The extracted values of $Q_\alpha(^{104}\mathrm{Te}) = 5.1(2)$ MeV and $Q_\alpha(^{108}\mathrm{Xe}) = 4.6(2)$ MeV are compared to the known even-even α emitters in the ^{100}Sn region, and to the analogous nuclei in the ^{208}Pb region, in Fig. 4. From Fig. 4 one can notice a nearly linear, increasing trend

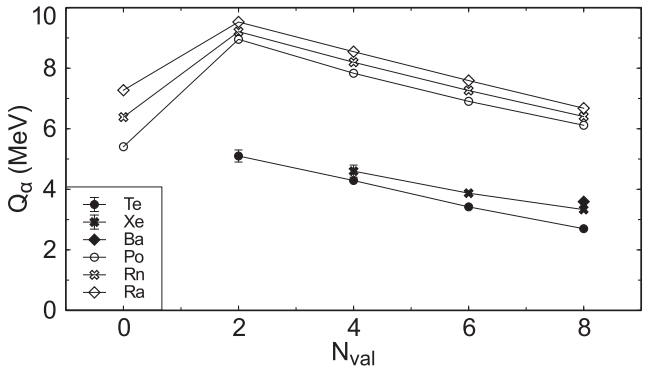

FIG. 4. Q_α values of the even-even α emitters in the ^{100}Sn region (solid symbols) and in the ^{208}Pb region (open symbols) as a function of the number of valence neutrons.

TABLE II. Properties of α-decay chains in even-even nuclei around ^{100}Sn, including the $N = Z$ chain from the present work. See the text and Fig. 5 for detailed discussion on W_α values.

Chain	Nuclide	E_α (keV)	$T_{1/2}$	b_α (%)	W_α
$N = Z$	^{108}Xe	4400(200)	58^{+106}_{-23} μs	100[a]	$\sim$3.7[b]
$N = Z$	^{104}Te	4900(200)	$<$18 ns	100[a]	$\gtrsim$13.1[c]
$N = Z + 2$	^{114}Ba	3480(20) [17]	380^{+190}_{-110} ms [17]	0.9(3) [35]	6^{+4}_{-3} [17]
$N = Z + 2$	^{110}Xe	3720(20) [17]	95^{+25}_{-20} ms [17]	64(35) [35]	$2.4^{+1.5}_{-1.6}$ [16]
$N = Z + 2$	^{106}Te	4128(9) [36]	70^{+20}_{-15} μs [17]	100 [35]	$4.4^{+1.2}_{-0.9}$ [17]
$N = Z + 4$	^{112}Xe	3216(7) [36]	2.7(8) s [37]	$0.8^{+1.1}_{-0.5}$ [36]	$3.4^{+4.7}_{-2.5}$ [36]
$N = Z + 4$	^{108}Te	3314(4) [20]	2.1(1) s [37]	49(4) [36]	2.7(3) [36]

[a]Assumed value.
[b]Obtained using the most likely E_α and $T_{1/2}$ values.
[c]Obtained using the most likely E_α and the 18-ns half-life limit.

towards the neutron shell closure in both cases. Once the $N = 126$ shell closure is reached, the Q_α values drop suddenly. The present data are in agreement with this linear trend, and therefore with the extrapolated values of $Q_\alpha(^{104}\text{Te}) = 5.053$ MeV and $Q_\alpha(^{108}\text{Xe}) = 4.440$ MeV [29]. Furthermore, the folding potential calculations [$Q_\alpha(^{104}\text{Te}) = 5.42(7)$ MeV and $Q_\alpha(^{108}\text{Xe}) = 4.65(15)$ MeV [19]] appear to reproduce well the present value for ^{108}Xe, but differ slightly from ^{104}Te. The mass excesses $\Delta(^{104}\text{Te}) = -49.8(4)$ MeV and $\Delta(^{108}\text{Xe}) = -42.8(4)$ MeV were obtained from the measured Q_α values and from the known masses of ^{100}Sn and ^{4}He [30]. Based on these masses and those of ^{102}Sn and ^{106}Te [30], two-proton decay Q values of $Q_{2p}(^{104}\text{Te}) = 0.6(4)$ MeV and $Q_{2p}(^{108}\text{Xe}) = 0.9(4)$ MeV were deduced. These are the first nuclei in the ^{100}Sn region with experimentally determined positive Q_{2p} values; however, in both cases $2p$ emission is dominated by α decay. The situation is different for ^{103}Te, where the α decay straddles the $N = 50$ shell closure, resulting in a much slower α decay. In fact, ^{103}Te has been proposed to be the best candidate for $2p$ emission in nuclei with $A > 100$ [31–33]. The ^{8}Be-emission Q value of 9.6(5) MeV was extracted for ^{108}Xe. While this is the largest value in the ^{100}Sn region, it is still too small to compete with α decay.

A useful quantity in the comparison of properties of α-emitting nuclei is the reduced decay width δ^2, which is defined as $\lambda_\alpha = \delta^2 P/h$, where λ_α is the partial α-decay constant, P is the Coulomb-barrier penetration factor, and h is Planck's constant. A standard way to obtain P for ground-state to ground-state α decay of even-even nuclei is to calculate the WKB integral [34], assuming s-wave α-particle emission. The quantity δ^2 is often given relative to ^{212}Po, $W_\alpha = \delta^2/\delta^2(^{212}\text{Po})$. The extracted W_α values, together with other properties of the new isotopes, are summarized and compared in Table II to those of previously known chains in even-even nuclei in the ^{100}Sn region.

Because of large energy uncertainties, W_α values are not tightly constrained for ^{104}Te and ^{108}Xe. Whereas it is not possible to deduce the individual α-particle energies with high precision, their sum of 9.29(9) MeV is better constrained. The $E_\alpha(^{108}\text{Xe})$ and $E_\alpha(^{104}\text{Te})$ energies and, thus, $W_\alpha(^{108}\text{Xe})$ and $W_\alpha(^{104}\text{Te})$ values are strongly correlated. This correlation can be found in Fig. 5, where the α-particle energies are varied within the present uncertainties, while keeping their sum constant. Solutions corresponding to the shaded area in Fig. 5 are excluded. Hence, solutions with $W_\alpha \lesssim 5$ for both ^{108}Xe and ^{104}Te are not likely, and at least for one of them $W_\alpha \gtrsim 5$, indicating superallowed character. This value is larger than for most of the neighboring nuclei, thus amplifying the increasing trend in preformation factors towards the $N = Z$ line.

Based on the α-decay systematics [15], it was concluded that the α-particle preformation factor of ^{104}Te is at least 3 times larger than that of ^{212}Po. Recently, a microscopic approach based on the multistep shell model predicted a factor of 4.85 enhancement for ^{104}Te [11], in fair agreement with the present data. In Ref. [12], the complex-energy

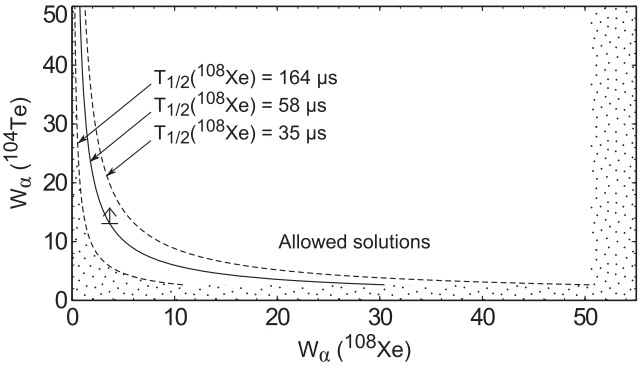

FIG. 5. The lower limit of $W_\alpha(^{104}\text{Te})$ as a function of that for ^{108}Xe, where the two α-particle energies are varied within $\pm$200 keV, while keeping their sum constant. The solid line corresponds to the most likely half-life of ^{108}Xe, whereas the dashed lines correspond to the upper and lower uncertainty limit. The shaded area is excluded by the present data. The data point marked with an arrow corresponds to the most likely $E_\alpha(^{108}\text{Xe})$ and $E_\alpha(^{104}\text{Te})$ values.

shell model was used and a preformation factor of ^{104}Te comparable to that of ^{212}Po was obtained, possibly pointing to the importance of proton-neutron interactions, which were not included in this latter calculation. The inclusion of the proton-neutron interaction was also necessary to reproduce the ^{212}Po α-decay lifetime [10].

In summary, the self-conjugate $^{108}\mathrm{Xe} \rightarrow {}^{104}\mathrm{Te} \rightarrow {}^{100}\mathrm{Sn}$ α-decay chain was observed for the first time. ^{104}Te is only the second instance of α decay to a doubly magic nucleus. The decay properties of ^{108}Xe and ^{104}Te indicate that the α-particle preformation factor, for at least one of these nuclei, is more than 5 times larger than that of ^{212}Po, suggesting superallowed α decay. This observation confirms the increasing trend of the preformation factor towards the $N = Z$ line, and provides the first quantitative information about this effect in self-conjugate nuclei, where it is expected to be strongest.

In order to stimulate further theoretical studies of the α-particle formation, and of the role of the proton-neutron interactions in particular, observation of more $^{108}\mathrm{Xe} \rightarrow {}^{104}\mathrm{Te} \rightarrow {}^{100}\mathrm{Sn}$ chains and reduction of uncertainties in neighboring α emitters are essential. A measurement of the ^{104}Te half-life is equally important, but will require a detection system sensitive to subnanosecond decay times. Observation of ^{112}Ba, a heavier $N = Z$ α emitter, is also possible.

This material is based upon work supported by the U.S. Department of Energy, Office of Science, Office of Nuclear Physics, under Contracts No. DE-AC02-06CH11357 (ANL), No. DE-FG02-94ER40834 (UMCP), No. DE-FG02-94ER40848 (UMass Lowell), No. DE-FG02-97ER41041 (UNC), and No. DE-FG02-97ER41033 (TUNL). This research used resources of ANL's ATLAS facility, which is a DOE Office of Science User Facility. C. S. acknowledges that this work has been supported by the Academy of Finland under the Finnish Center of Excellence Programme (Contract No. 284612).

*kauranen@anl.gov
†Present address: Department of Physics, United States Naval Academy, Annapolis, Maryland 21402, USA.
‡Present address: Universitá degli Studi di Milano and INFN, Via Celoria 16, I-20133 Milano, Italy.
§Present address: U.S. Army Research Laboratory, Adelphi, Maryland 20783, USA.
‖Present address: GSI, Planckstraße 1, D-64291, Darmstadt, Germany.
¶Present address: University of Surrey, Guildford GU2 7XH, United Kingdom.
**Present address: Department of Physics and Applied Physics, University of Massachusetts Lowell, Lowell, Massachusetts 01854, USA.

[1] J. Erler, N. Birge, M. Kortelainen, W. Nazarewicz, E. Olsen, A. M. Perhac, and M. Stoitsov, Nature (London) **486**, 509 (2012).
[2] T. Faestermann, M. Górska, and H. Grawe, Prog. Part. Nucl. Phys. **69**, 85 (2013).
[3] C. B. Hinke *et al.*, Nature (London) **486**, 341 (2012).
[4] D. Seweryniak, M. P. Carpenter, S. Gros, A. A. Hecht, N. Hoteling, R. V. F. Janssens, T. L. Khoo, T. Lauritsen, C. J. Lister, G. Lotay, D. Peterson, A. P. Robinson, W. B. Walters, X. Wang, P. J. Woods, and S. Zhu, Phys. Rev. Lett. **99**, 022504 (2007).
[5] I. G. Darby, R. K. Grzywacz, J. C. Batchelder, C. R. Bingham, L. Cartegni, C. J. Gross, M. Hjorth-Jensen, D. T. Joss, S. N. Liddick, W. Nazarewicz, S. Padgett, R. D. Page, T. Papenbrock, M. M. Rajabali, J. Rotureau, and K. P. Rykaczewski, Phys. Rev. Lett. **105**, 162502 (2010).
[6] A. Florescu and A. Insolia, Phys. Rev. C **52**, 726 (1995).
[7] S. Kumar, D. Bir, and R. K. Gupta, Phys. Rev. C **51**, 1762 (1995).
[8] S. Kumar and R. K. Gupta, Phys. Rev. C **49**, 1922 (1994).
[9] R. G. Lovas, R. J. Liotta, A. Insolia, K. Varga, and D. S. Delion, Phys. Rep. **294**, 265 (1998).
[10] K. Varga, R. G. Lovas, and R. J. Liotta, Phys. Rev. Lett. **69**, 37 (1992).
[11] M. Patial, R. J. Liotta, and R. Wyss, Phys. Rev. C **93**, 054326 (2016).
[12] R. I. Betan and W. Nazarewicz, Phys. Rev. C **86**, 034338 (2012).
[13] R. D. Macfarlane and A. Siivola, Phys. Rev. Lett. **14**, 114 (1965).
[14] D. Seweryniak, K. Starosta, C. N. Davids, S. Gros, A. A. Hecht, N. Hoteling, T. L. Khoo, K. Lagergren, G. Lotay, D. Peterson, A. Robinson, C. Vaman, W. B. Walters, P. J. Woods, and S. Zhu, Phys. Rev. C **73**, 061301 (2006).
[15] S. N. Liddick *et al.*, Phys. Rev. Lett. **97**, 082501 (2006).
[16] Z. Janas, C. Mazzocchi, L. Batist, A. Blazhev, M. Górska, M. Kavatsyuk, O. Kavatsyuk, R. Kirchner, A. Korgul, M. La Commara, K. Miernik, I. Mukha, A. Plochocki, E. Roeckl, and K. Schmidt, Eur. Phys. J. A **23**, 197 (2005).
[17] L. Capponi *et al.*, Phys. Rev. C **94**, 024314 (2016).
[18] C. N. Davids and J. D. Larson, Nucl. Instrum. Methods Phys. Res., Sect. B **40–41**, 1224 (1989).
[19] P. Mohr, Eur. Phys. J. A **31**, 23 (2007).
[20] F. Heine, T. Faestermann, A. Gillitzer, J. Homolka, M. Köpf, and W. Wagner, Z. Phys. A **340**, 225 (1991).
[21] S. Hofmann *et al.*, Eur. Phys. J. A **48**, 62 (2012).
[22] S. Hofmann, G. Münzenberg, K. Valli, F. P. Heßberger, J. R. H. Schneider, P. Armbruster, B. Thuma, and Y. Eyal, GSI Sci. Rep. **1982-1**, 241 (1982).
[23] K. H. Schmidt, C. C. Sahm, K. Pielenz, and H. G. Clerc, Z. Phys. A **316**, 19 (1984).
[24] T. Faestermann, A. Gillitzer, K. Hartel, W. Henning, and P. Kienle, AIP Conf. Proc. **164**, 675 (1987).
[25] M. D. Sun *et al.*, Phys. Lett. B **771**, 303 (2017).
[26] G. Audi, *et al.*, Chin. Phys. C **41**, 030001 (2017).
[27] https://physics.nist.gov/PhysRefData/Star/Text/intro.html.
[28] M. J. Berger, M. Inokuti, H. H. Andersen, H. Bichsel, D. Powers, S. M. Seltzer, D. Thwaites, and D. E. Watt, J. Int. Comm. Radiat. Units Meas. **os25**, NP (1993).
[29] C. Xu and Z. Ren, Phys. Rev. C **74**, 037302 (2006).
[30] M. Wang, G. Audi, F. G. Kondev, W. J. Huang, S. Naimi, and X. Xu, Chin. Phys. C **41**, 030003 (2017).

[31] E. Olsen, M. Pfützner, N. Birge, M. Brown, W. Nazarewicz, and A. Perhac, Phys. Rev. Lett. **110**, 222501 (2013).
[32] E. Olsen, M. Pfützner, N. Birge, M. Brown, W. Nazarewicz, and A. Perhac, Phys. Rev. Lett. **111**, 139903(E) (2013).
[33] S. Hofmann, Radiochim. Acta **70-71**, 93 (1995).
[34] J. O. Rasmussen, Phys. Rev. **113**, 1593 (1959).
[35] C. Mazzocchi, Z. Janas, L. Batist, V. Belleguic, J. Döring, M. Gierlik, M. Kapica, R. Kirchner, G. A. Lalazissis, H. Mahmud, E. Roeckl, P. Ring, K. Schmidt, P. J. Woods, and J. Żylicz, Phys. Lett. B **532**, 29 (2002).
[36] R. D. Page, P. J. Woods, R. A. Cunningham, T. Davinson, N. J. Davis, A. N. James, K. Livingston, P. J. Sellin, and A. C. Shotter, Phys. Rev. C **49**, 3312 (1994).
[37] D. Schardt, R. Kirchner, O. Klepper, W. Reisdorf, E. Roeckl, P. Tidemand-Petersson, G. Ewan, E. Hagberg, B. Jonson, S. Mattsson, and G. Nyman, Nucl. Phys. **A326**, 65 (1979).